Lactate measurement by neurochemical profiling in the dorsolateral prefrontal cortex at 7T: accuracy, precision and relaxation times

Masoumeh Dehghani[1], Kim Q. Do[1], Pierre Magistretti[1,3,4] , Lijing Xin[2]

1. Center for Psychiatric Neuroscience (CNP), Department of Psychiatry, Lausanne University Hospital - CHUV, Prilly-Lausanne, Switzerland.
2. Animal Imaging and Technology Core (AIT), Center for Biomedical Imaging (CIBM), Ecole Polytechnique Fédérale de Lausanne, Lausanne, Switzerland
3. BESE Division, King Abdullah University of Science and Technology, Thuwal, Saudi Arabia
4. Brain Mind Institute, Ecole Polytechnique Fédérale de Lausanne, Lausanne, Switzerland.

Running title: Lactate measurement at 7T: accuracy, precision, relaxation times

Corresponding author:

Lijing Xin, Ph.D., EPFL ENT-R CIBM-AIT, Station 6, CH-1015 Lausanne, Switzerland

lijing.xin@epfl.ch

Tel. + 41 21 693 0597

Fax + 41 21 693 7960

Word count: 5803

Abstract

Purpose: This assesses the potential of measuring lactate in the human brain using three non-editing MRS methods at 7T and compares the accuracy and precision of the methods.

Methods: ^{1}H MRS data were measured in the right dorsolateral prefrontal cortex using a semi-adiabatic SPECIAL sequence with three different protocols: I. TE = 16ms; II. TE = 110ms; and III. TE = 16ms, TI = 300ms. T_1 and T_2 relaxation times of lactate were also measured. Simulated spectra were generated for three protocols with known concentrations, using a range of spectral linewidths and signal-to-noise ratios to assess the effect of data quality on the measurement precision and accuracy.

Results: Lactate was quantified in all three protocols with mean CRLB of 8%(I), 13%(II), and 7%(III). The T_1 and T_2 relaxation times of lactate were 1.9±0.2s and 94±13ms, respectively. Simulations predicted a spectral linewidth-associated underestimation of lactate measurement. Simulations, phantom and *in vivo* results showed that protocol II was most affected by this underestimation. In addition, the estimation error was insensitive to a broad range of spectral linewidth with protocol I. Within-session CVs of lactate were $6.1 \pm 7.9\%$(I) , $22.3 \pm 12.3\%$(II) and $5.1 \pm 5.4\%$(III), respectively.

Conclusion: We conclude that protocol I and III have the potential to measure lactate at 7T with good reproducibility, while the measurement accuracy and precision depend on spectral linewidth and SNR, respectively. Moreover, simulation is valuable for the optimization of measurement protocols in future study design and the correction for measurement bias.

Keywords: spin-echo full-intensity acquired localized (SPECIAL), MRS, lactate, short TE, inversion, T_1 and T_2 relaxation times

Introduction

Lactate, a metabolic product of glycolysis, an intermediate in the energy metabolism of carbohydrate-consuming organs, such as the brain [1-3], has been recently shown to play a critical role in neuroplasticity and neuroprotection [4]. Progressive increases in lactate uptake and metabolism in the brain has been reported during physical exercise [5,6], neuronal activation [7,8], and other changes in physiological state [9,10]. Lactate abnormalities are implicated in psychiatric conditions such as bipolar disorder [11-14], major depression [15], panic disorder [16,17], schizophrenia [18], and other brain pathological states, including mitochondrial dysfunction [19], tumors [20] and ischemia [21].

In vivo measurement of lactate by MRS is challenging due to its low abundance in the brain (~1 mM) [22,23] and restricted spectral resolution, limiting its distinction from overlapping macromolecular signals at 1.2 ppm. A number of spectral editing techniques, such as J-difference editing [24-26] and double-quantum filters [27], have been proposed to achieve measurement of lactate without contamination from macromolecules. However, important information on other metabolites is generally sacrificed, and prior knowledge of relaxation dynamics is additionally required for quantification of data acquired with these methods.

Short-TE (< 20ms) MRS offers high sensitivity with minimal signal loss from T_2 relaxation and scalar coupling evolution. With further enhancement in sensitivity and spectra dispersion at 7 T, many studies [23,28-32] have demonstrated the potential of short-TE MRS for providing important insight in the neurochemical profile, including lactate and other metabolites and neurotransmitters implicated in psychiatric and neurological disorders. For example, alteration in glutamate, glutamine, glutathione and γ-aminobutyric acid has been reported in schizophrenia, suggesting impaired NMDA receptor signaling and oxidative stress[33]. Increased lactate, glutamate, glutathione and decreased glutamine have been observed during visual stimulation[34]. Changes in lactate and glutamate has been consistently observed during other neuronal stimuli[35], underscoring their important roles in neuronal activity. Therefore, the simultaneous measurement of these metabolites may assist in offering a more comprehensive understanding of neurochemical mechanisms underlying psychiatric disorders or neuronal activities. Nevertheless, due to spectral overlap and the presence of broad macromolecular signals, metabolite quantification generally relies on deconvolution methods implemented in software applications such as LCModel [36] and jMRUI [37]. The quantification accuracy and precision requires further validation.

To achieve clear detection of lactate along with the measurement of other metabolites of interest, one can also perform an experiment at long TE or by inversion-recovery based on the large differences in T_1 and T_2 relaxation times between lactate and macromolecules. At long-TE (~ 1/J), macromolecular signals are

minimized due to their short T_2 and lactate appears as a characteristic negative doublet. At 7 T with a TI of 300 ms, macromolecular signals are minimized around their zero-crossing point, while lactate still has a negative phase due to its slower T_1 relaxation [38]. However, increasing the echo time or using inversion recovery typically results in loss of SNR due to the T_1 or T_2 relaxation effects [39,40].

The dorsolateral prefrontal cortex, a key region for cognitive function, has been strongly suggested to be altered in main psychiatric disorders such as schizophrenia[41–43], bipolar disorders and depression[44]. Functional imaging studies have shown DLPFC hypoactivity in depression ([44] and references therein). Additionally, altered expression of genes encoding proteins involved in the synaptic activity, NMDA receptor activity and energy metabolism are noted in the DLPFC in schizophrenia [42,45] and bipolar disorder.

We thus aimed to assess and compare three ^{1}H MRS approaches (short TE, long TE and inversion recovery) for simultaneous neurochemical profiling in the DLPFC of the human brain at 7 T, with a focus on the accuracy and precision of the lactate measurement. In addition, to correct for relaxation effects on the lactate signal, T_1 and T_2 relaxation times of lactate were also measured.

Methods

In vivo experiments

MR experiments were performed on a 7 T/68 cm MR scanner (Siemens Medical Solutions, Erlangen, Germany) using a commercial transmit birdcage coil with 32-channel receive array (Nova Medical Inc., Wilmington, MA, USA). All volunteers provided informed consent prior to the study.

To alleviate the limitations imposed on B_1 in the peripheral region of the brain, a dielectric pad [23,46] was placed above the right hemisphere of scalp covering the DLPFC. To position the voxel of interest (VOI = $30 \times 15 \times 15$ mm^3) in the right DLPFC of the brain, three-dimensional T_1-weighted images were acquired using magnetization prepared 2 rapid acquisition gradient echoes (MP2RAGE) [47] with acquisition parameters of TE/TR = 4.94/6000 ms, TI_1/TI_2 = 800/2700 ms, voxel size = $0.6 \times 0.6 \times 0.6$ mm^3, matrix size = $320 \times 320 \times 256$. B_o field inhomogeneities were minimized over the VOI by adjusting the first and second-order shim terms using FAST(EST)MAP [48]. ^{1}H MR spectra were acquired with the three different acquisition protocols from the VOI using the semi-adiabatic spin-echo full-intensity localized spectroscopy (sSPECIAL) sequence [38]. To minimize the unwanted signal from outside the VOI, outer volume suppression (OVS) was applied along six saturation bands around the VOI. Furthermore, water signal was suppressed using variable power radiofrequency pulses with optimized relaxation delays (VAPOR) [49] prior to the localization.

Seven subjects (24 ± 5 years, 3 females/4 males) participated in experiments of *in vivo* lactate measurement using three different protocols with the same total acquisition time. Data acquisition parameters, including TR of 6.5 s, spectral bandwidth of 6000 Hz, 100 averages (2 averages × 50 blocks) and 2048 sampling points were kept the same between the three protocols except for TE and TI, which were set as follows: protocol I. TE = 16 ms, no inversion; protocol II. TE = 110 ms, no inversion; protocol III. TE = 16 ms, TI = 300 ms. The 110 ms TE used in protocol II was determined with the following considerations: 1) at TE of 110ms, the inverted signal intensity of lactate is similar to that at TE of 144 ms (1/J) (Supporting Information Figure S1, evolution of signal intensity with TE including effects of J-evolution and T_2 relaxation); 2) a shorter TE (110 vs 144ms) to minimize T_2 relaxation signal loss for other metabolites. Based on the macromolecule T_1 value determined previously at 7T [38], a TI of 300 ms, previously estimated to be the nulling point of macromolecule signal, was used in protocol III. These three protocols were applied in a random order between subjects to avoid potential bias from the spectral quality changing over time. The linewidths of total creatine were evaluated for the three protocols and compared by one-way ANOVA. In addition, unsuppressed water spectra acquired at TE = 16 ms were used as internal references for obtaining apparent metabolite concentrations (in institutional unit, without relaxation correction).

To correct for relaxation effects on the estimation of lactate concentration by protocol II and III, T_1 and T_2 relaxation times of lactate in the DLPFC were measured in six subjects (23 ± 3 years, 2 females/4 males). To measure T_1, spectra were acquired using the semi-adiabatic SPECIAL sequence with inversion-recovery at different TIs (50, 300, 1300, 2200, and 4000 ms) and one additional scan was performed without the inversion pulse (TI$_{off}$ in Eq. 1). To measure T_2, spectra were acquired using semi-adiabatic SPECIAL sequence with different TEs (16, 110 and 240 ms). The number of data points was determined to reach adequate measurement points within 1h time frame for each session.

Post-processing procedure

Frequency drift and phase correction were applied prior to summation of multi-block spectra using an in-house Matlab program. LCModel was employed for the quantification of metabolites using basis sets generated for each protocol. The density matrix formalism [38,50] was used to generate the basis sets in Matlab (MathWorks, Natick, MA, USA). Metabolite spectra included alanine, ascorbate, aspartate, creatine, glucose, glycerophosphocholine, glycine, glutamate, glutamine, glutathione, lactate, myo-inositol, N-acetylaspartate (NAA), N-acetylaspartylglutamate, phosphocholine, phosphocreatine, phosphoethanolamine, serine, scyllo-inositol, taurine, and γ-aminobutyric acid. For protocol II and III, the CH_3 and CH_2 groups of creatine, phosphocreatine and N-acetylaspartate were prepared as two separate metabolites in their basis sets, due to the difference in signal intensity at 110 ms TE and 300 ms TI

resulting from different relaxation rates of those chemical groups. The macromolecule spectrum previously measured *in vivo* was incorporated in the basis sets for protocols I and III [51]. For basis set of protocol II, additional macromolecule spectra were measured from two subjects using the semi-adiabatic SPECIAL sequence with TI of 950 ms (previously determined at 7T [51]) and TE of 110 ms. Minor residual metabolites resonances including those of total creatine, choline, NAA and glutamate, were removed in jMRUI [52]. The macromolecule spectrum for each protocol was incorporated in their basis set as one individual component with the other metabolites and the built-in macromolecule-fitting function was disabled in LCModel by setting NSIMUL = 0 in the control file. The analysis window in LCModel was over the chemical shift range of 0.4 to 4.1 ppm. All metabolites with CRLB of 999% were considered as non-detectable. Spectral SNR was calculated as the maximum peak height of the NAA singlet at 2.01 ppm divided by the standard deviation of noise between 11 and 12 ppm.

To estimate the T_1 relaxation time of lactate, the apparent concentrations of lactate at different TIs (S(TI)) were fitted versus their corresponding TIs using the following equation :

$$S(TI) = S(TI_{off}) \cdot \left(1 - (1+\alpha) \cdot e^{\frac{-TI}{T_1}} + \alpha \cdot e^{\frac{-6.5}{T_1}} \right) / \left(1 - e^{\frac{-6.5}{T_1}} \right) \qquad (1)$$

α represents the factor for flip angle of the inversion pulse. $S(TI_{off})$ represents the signal intensity at TE of 16 ms without inversion.

To account for different spectral patterns due to J-modulation at the three TEs used for T_2 measurement, we used TE-specific basis sets simulating the metabolite spectral pattern for each TE. After LCModel quantification, the obtained apparent concentrations will decay with TE as a function of apparent T_2. These apparent concentrations of lactate at different TE were then fitted using $S(TE) = S_0 \cdot e^{-TE/T2}$ to calculate the apparent T_2 of lactate.

Lactate concentrations were corrected for T_1 and T_2 relaxation; briefly, apparent concentrations were divided by $e^{-TE/T2} \cdot (1 - e^{-TR/T1})$ for protocol I and II, by $e^{-TE/T2} \cdot (1 - 2 \cdot e^{-TI/T1} + e^{-TR/T1})$ for protocol III.

Monte Carlo Simulation

The accuracy and precision of acquisition protocols I, II, and III in MRS detection of lactate were explored further by Monte Carlo simulation. Synthesized MR spectra consisted of 21 metabolites simulated in Matlab (MathWorks, Natick, MA, USA) using the density matrix formalism, assuming an ideal double spin-echo at the TEs used in each protocol. To take into account the potential differences in T_1 and T_2 relaxation of individual resonances in NAA, creatine, and phosphocreatine [38,53] in protocols II and III , NAA was split into methyl and aspartate moieties, creatine and phosphocreatine were treated as

two separate peaks of CH_3 and CH_2. Final simulated spectra were generated by combining experimentally measured macromolecule spectra with all metabolite spectra using the mean apparent concentrations measured in this study for each protocol shown in Table 1. Literature values [54,55] were used for those metabolites which were not detected (CRLB=999%) in protocol I. For non-detectable metabolites in protocol II and III, relaxation effects was applied on the values taken from protocol I assuming a T_1 of 1.2s [38] and a T_2 of 110ms[53].

To generate spectra at different spectral conditions, spectral linewidths were varied from 3 to 17 Hz in steps of 1 Hz. Normally-distributed random noise was added to the simulated spectra to create a range of different SNR (25-500). For a given spectral linewidth and SNR, 100 spectra were generated with different noise seeds. Overall, every combination of 15 different linewidth values (ranging from 3 to 17 Hz in step of 1 Hz) and 16 different SNR values (ranging from 25 to 300 in step of 25 and from 300 to 500 in step of 50) results in generating 24 000 simulated spectra. All simulated spectra were further analyzed by LCModel.

Accuracy and reproducibility assessment

To assess how closely the estimated concentration of lactate from LCModel output $C_{est}(i)$ matches its actual input concentration, C_{act}, used in simulation, the mean estimation error (%EE) was calculated using the following equation [54] :

$$\% EE = \frac{1}{N} \sum_{i=1}^{N} \frac{C_{est}(i) - C_{act}}{C_{act}} \times 100 \tag{2}$$

where N refers to the total number of simulations per experimental conditions (N = 100).

To check how well the acquisition protocols will return the same value for lactate concentration at different spectral conditions, the reproducibility error (RE), a component of precision in measurement, was determined by the following equation:

$$\% RE = \frac{\sqrt{\frac{\sum_{i=1}^{N}(C_{est}(i) - \overline{C_{est}})^2}{N-1}}}{\overline{C_{est}}} \times 100 \tag{3}$$

where $\overline{C_{est}}$ is the mean of estimated concentration in simulated spectra at a given experimental condition.

It should be noted that REs calculated from simulations suggest the measurement precision of the current quantification setting with spectral noise and linewidth as main contributors to variance.

To evaluate within-session reproducibility, *in vivo* data for each protocol were spitted into two sub-sessions, which were analyzed respectively for the calculation of within-session coefficient of variance (CV).

To assess the effect of SNR on the reproducibility of *in vivo* lactate measurement, three blocks of data containing 20, 40, and 60 spectra from the same subjects were created for each protocol and analyzed with LCModel.

Phantom experiments

To further validate the accuracy of lactate measurement by three protocols, additional experiments were performed on phantoms containing 0, 0.2, 0.4, 0.6 and 1 mM of lactate. These phantoms were prepared with phosphate buffer saline, 4% of bovine serum albumin (BSA) for mimicking the macromolecule spectrum and 4mM of creatine for frequency referencing in LCModel quantification. All chemicals were ordered from Sigma-Aldrich Chemie GmbH, Buchs, Switzerland.

[1]H MR spectra were acquired in these phantoms using three protocols as used *in vivo,* except that TR was extended to 15s and VOI was 20 x 20 x 25mm^3. Unsuppressed water spectra were acquired for quantification and eddy current correction.

The mean linewidth of water in phantoms is 3.5Hz, therefore, 10Hz linebroadening was applied to spectra for mimicking the similar spectral linewidth *in vivo*. To generate the basis set for BSA quantification in phantom measurements, spectra were acquired using three protocols from a phantom containing simply BSA and 3-(Trimethylsilyl)propionic-2,2,3,3-d4 acid sodium salt (TSP). In the control file, atth2o was set to 1 and wconc was set to 55556. T_1 and T_2 relaxations of lactate in the phantom is 1647ms (R^2=0.999) and 322ms (R^2=0.944). Lactate concentrations measured by three protocols were corrected for relaxation effects. To evaluate the measurement accuracy, linear regression was performed between the true and measured lactate concentrations in the phantom. To study the effect of linewidth and SNR on the measurement accuracy, phantom data with lactate of 0.6mM were further analyzed with different linebroadening (0 - 10 Hz, 1Hz/step) and different number of averages.

Statistics

The comparison of values measured by the three protocols was performed using one-way ANOVA with Bonferroni's multiple comparison test in Graphpad Prism 5 (Graphpad Software, San Diego, CA, USA). CV was calculated using standard deviation of measured values divided by their mean value.

Results

B_0 shimming over the voxel positioned in the right DLPFC (Figure 1) yielded water spectra with linewidth of 13.5 ± 1.0 Hz and a total creatine linewidth of 10.8 ± 1.7 Hz in water-suppressed spectra (n = 7). *In vivo* water suppressed spectra for neurochemical profiling were acquired using the semi-adiabatic SPECIAL sequence with three acquisitions protocols consisting of I. TE = 16 ms, no inversion; II. TE = 110 ms, no inversion; and III. TE = 16 ms, TI = 300 ms (Figure 2). With the total acquisition time of 10 min, spectra acquired using protocol I had a SNR of 330 ± 50 and the spectra acquired using protocols II and III had lower SNRs of 145 ± 30 and 150 ± 30, respectively. The linewidths of total creatine for the three protocols were highly consistent (p = 0.93), with 10.7 ± 1.7 Hz (protocol I), 10.7 ± 1.4 Hz (protocol II) and 11.0 ± 2.2 Hz (protocol III). The good spectral quality from each protocol together with effective water and outer volume suppression, allowed the quantification of a significant number of metabolites, including lactate, as shown in Table 1.

The spectral pattern varied across the acquisition protocols. As expected, the highest SNR was achieved when using protocol I with lactate sitting on the right shoulder of macromolecular resonances (Figure 2A). Due to rapid T_2 relaxation decay, signal intensities of macromolecules were largely attenuated in the spectra from protocol II. Both lactate and macromolecules underwent J-evolution, resulting in spectral patterns with negative phases and a distinct lactate peak (Figure 2B). Spectra from protocol III showed significant signal loss due to T_1 relaxation, with the macromolecular signal passing through the zero-crossing point, and a well-defined negative lactate methyl peak (Figure 2C). Lactate was quantified reliably in all three protocols with mean CRLB of 8 % (protocol I), 13 % (protocol II), and 7 % (protocol III).

The T_1 and T_2 relaxation times of lactate were determined *in vivo* in the right DLPFC as 1.9 ± 0.2 s ($R^2 = 0.986$) and 94 ± 13 ms ($R^2 = 0.973$), respectively. After T_1 and T_2 relaxation correction, the lactate concentration was determined as 0.67 ± 0.10 (protocol I), 0.57 ± 0.16 (protocol II) and 0.66 ± 0.09 (protocol III) (Figure 3). The CVs across seven subjects were 15% for protocol I, 28% for protocol II, and 13% for protocol III, respectively. There is no significant difference between lactate values estimated through three protocols I, II and III (p = 0.25). However, the mean lactate value of protocol II were 15% lower than those estimated from protocol I and III.

To investigate the impact of SNR on the estimated concentrations and CRLBs, three sub-spectra (averages of 20, 40 and 60) were generated for each protocol. SNRs ranged from 185 to 318 for protocol I, 80 to 141 for protocol II, and 88 to 155 for protocol III. Estimated lactate levels were not significantly different for three SNRs within each protocol (protocol I: p =0.99, protocol II: p = 0.93, protocol III: p = 0.89, Figure

4A). In addition, the CRLBs did not change significantly with the increase of SNR for protocol I (p = 0.49), but they reduced by ~30 % in protocol II and III from 20 to 60 averages (protocol II: p = 0.09, protocol III: p = 0.07) (Figure 4B).

Representative LCModel fits of glutamate, glutamine, glutathione and γ-aminobutyric acid were shown in Figure 2. Glutamate was quantified in all three protocols with a mean CRLB of 2 %. Glutamine and glutathione were quantified with smaller mean CRLBs in protocol I and III (6-9 %) relative to protocol II (12-16%). The mean CRLB of γ-aminobutyric acid was about 13-15 % in all three protocols (Table 1).

To evaluate the accuracy and precision of the lactate measurement, Monte Carlo simulations were performed and proton spectra were simulated using double spin-echo sequence for protocols I, II and III, with spectral linewidths ranging from 3 to 17 Hz and SNRs ranging from 25 to 500. Figure 5 depicts a series of simulated spectra with spectral linewidths of 3, 5, 11, 17 Hz, and SNRs of 300 for protocol I and 150 for protocol II and III. LCModel fits of macromolecules, spline baseline and lactate are also shown for every spectral condition.

The contour plots in Figure 6A illustrate the mean EE of lactate as a function of linewidth and SNR. Similar patterns were observed in variations of EE with linewidth and SNR in all three protocols. In general, an underestimation of lactate values was observed. The mean EE varies mainly with linewidth when SNR is above a given value (~100) and the narrower the linewidth, the more accurate the measurement. The slope of mean EE variations relative to linewidth at experimental SNR for protocol I (SNR=300), protocols II and III (SNR=150) demonstrated that protocol I was less sensitive to the linewidth variations relative to the other two protocols (Figure 7). Under the experimental conditions, EE (mean ± SD) was -12 ± 5% in protocol I (LW = 11 Hz and SNR = 300) and increased to -26 ± 6% in protocol II (LW = 11 Hz and SNR = 150) and -14 ± 4% in protocol III (LW = 11 Hz and SNR = 150).

Figure 6B and Figure 6C illustrate the RE and CRLB of lactate measurements as a function of linewidth and SNR. Contour plots of RE and CRLB followed the same pattern in all three protocols and were mainly influenced by the SNR of the spectra. Lactate was estimated with a RE of 5% and CRLB of 7% in protocol I, RE of 8% and CRLB of 11% in protocol II, RE of 5% and CRLB of 9% in protocol III at the experimental conditions.

Additional experiments were performed on phantoms with different lactate levels to further validate the accuracy of lactate measurement. BSA is a macromolecule (~ 66kDa) contains many amino acids such as valine, lysine, threonine, histidine, alanine, etc [56]. The phantoms with BSA produced a similar broad spectrum mimicking the *in vivo* macromolecule spectrum. Examples of phantom spectra acquired using three protocols, fits of BSA and lactate were shown (Supporting Information Figure S2). Measured

phantom lactate concentrations by three protocols were compared with true lactate concentrations in phantoms. Using linear regression, slopes of 0.87(R^2=0.9947), 0.69 (R^2=0.9968) and 0.83(R^2=9688) were obtained for protocol I, II and III, respectively (Figure 8A). Overall, lactate levels were underestimated by all three protocols. The underestimation was similar for both protocol I and III but more pronounced for protocol II. When there is no lactate in the phantom, LCModel reported 0.004 mM (CRLB = 274%) for protocol I, 0.014 mM (CRLB = 76%) for protocol II and 0 mM (CRLB = 999%) for protocol III. As predicted by simulations, the measurement accuracy depends more on spectral linewidth. In Figure 8B, measured lactate levels in the phantom also showed similar dependency on the spectral linewidth. Figure 8C showed that measurement accuracy is insensitive to SNR once sufficient SNR is reached.

The within-session reproducibility was evaluated by CVs and the results were shown in Table 2. Both protocol I and III exhibit good reproducibility for lactate with CVs of 6.1 ± 7.9% and 5.1 ± 5.4%, respectively. Among three protocols, protocol II showed the highest CVs for Lac, Glu and Gln. For GABA, protocol I (11.7 ± 8.4%) has the best reproducibility and then protocol II (16.5 ± 9.6%), while protocol III had the poorest (39.2 ± 32.2%).

Furthermore, the spectral linewidth and SNR dependence of mean EE, RE, and CRLB in the estimation of glutamate, glutamine, glutathione, and γ-aminobutyric acid for the three protocols were also shown (Supporting Information, Figure S3-5). Contour plots of EE, RE and CRLB for glutamate are similar for different protocols, namely the EE is more sensitive to linewidth, RE and CRLB are more sensitive to SNR. The patterns of EE for glutamine, glutathione, and γ-aminobutyric acid are different between different protocols. RE and CRLB for glutamine and glutathione depend more on SNR than on linewidth in all three protocols. The dependency of RE and CRLB of γ-aminobutyric acid on linewidth and SNR is complicated and different between three protocols. Under *in vivo* experimental conditions, the RE and CRLB of Glu and GABA measurement are comparable between three protocols. However, for Gln and GSH, protocol II has substantially higher RE and CRLB comparing to protocol I and III.

Discussion

In this study, we focused on investigating lactate measurement at 7T by three protocols for neurochemical profiling (I. TE = 16 ms, II. TE = 110 ms and III. TE/TI = 16/300 ms). We showed that simulations predicted a general underestimation of lactate measurement and it was consistent with the *in vivo* and phantom results that this underestimation was to the most extent for protocol II. Furthermore, lactate can be quantified by all three protocols with mean CRLB of 7-13% and mean within-session CVs of 5-6% (protocol I and III) and 20% (protocol II). The measurement accuracy was largely associated with spectral linewidth, while CRLB and RE were more associated with SNR.

The estimated lactate concentrations *in vivo* by protocols I, II and III were 0.67 ± 0.10, 0.57 ± 0.16 and 0.66 ± 0.09, respectively. The values from protocol II were lower than those measured by other two protocols. This was in good agreement with the respective estimation errors of $-12 \pm 5\%$, $-26 \pm 6\%$ and $-14 \pm 4\%$ predicted from simulations of the three protocols under *in vivo* experimental conditions, with protocol II yielding the most underestimated values. If one corrects the *in vivo* values with the estimated errors predicted by simulation, the lactate values are 0.75 ± 0.12 (protocol I), 0.76 ± 0.22 (protocol II) and 0.77 ± 0.11 (protocol III), which are in excellent agreement ($p = 0.99$). Phantom results (Figure 8A) suggested approximately 13%, 21% and 17% underestimation for protocol I, II and III, respectively, which was consistent with EEs estimated by simulations. Such consistency advocates that simulations could correctly predict the measurement accuracy and be used for correcting measurement bias for in vivo measurements.

The within-session CVs of protocol I and III were $6.1 \pm 7.9\%$ and $5.1 \pm 5.4\%$, which were lower than the CVs (12-24%) measured by a J-difference editing technique in the striatum[57], suggesting that good reproducibility can be achieved without spectral editing for lactate. However, CV of 22.3 ± 12.3 % for protocol II is the poorest among three protocols, which may be ascribed to the dramatic signal loss with T_2 relaxation.

Both simulation and phantom results showed that the measurement accuracy is largely related to spectral linewidth. The general underestimation of lactate existing in all protocols is likely attributable to the overestimation of spline baseline with the increase in linewidth. As shown in Figure 5, the spline baseline becomes less flat with the increase of linewidth, and part of the lactate signal may be assigned to the baseline, leading to an underestimation. Since most studies perform comparisons between groups, matched spectral quality between groups, particularly for linewidth, would minimize systematic error originated from the quantification bias. Furthermore, EE is less sensitive to linewidth variations with protocol I than the others over a broad range of linewidth values (Figure 7), suggesting that short-TE MRS is a more sensitive method to detect lactate alterations in group comparison applications and for correlating with other parameters. However, for these common analyses, linewidth variation within experimental samples should be carefully inspected when using protocols II or III. Finally, the simulation results may also serve as a look-up table for correction factors at a given spectral condition.

In protocols II and III, macromolecular resonances were minimized and the methyl resonance of lactate was more clearly resolved relative to protocol I, where lactate was on the right shoulder of macromolecular resonances. However, both *in vivo* measurements and simulations showed consistent results that protocol I had CRLBs ($8 \pm 1\%$) comparable to protocol III ($7 \pm 1\%$) and lower than protocol II ($13 \pm 3\%$), suggesting that short-TE spectra with quantitation by LCModel can reliably measure lactate

despite the presence of underlying macromolecule resonances. This may be attributed to the association between SNR and CRLB consistently seen in within-session *in vivo* data (Figure 4B) and simulation results (Figure 6C). With the same acquisition time, SNR is doubled for protocol I relative to protocol II and III, which likely mitigates the effect of the spectral overlap on the measurement reliability. In addition, the analysis of sub-spectra with different SNR (Figure 4B) demonstrated that CRLBs remained approximately the same when SNR decreased by a factor of two in protocol I, while CRLB increased by 30% in protocol II and III. This suggests that the acquisition time can be substantially shortened when using protocol I, which is critical for patient studies with limited time. For example, within-session data showed that a 2.2-min scan of protocol I (20 averages) can achieve a SNR of 180 and CRLB of 9 ± 1 %, which is smaller than CRLB of 15 ± 5 % obtained by protocol II and similar to 7 ± 2% by protocol III with 3 fold the scanning time.

Note that lactate measured by all three protocols in this study may contain signal contribution from the threonine methyl resonance, which has a similar chemical shift and J-coupling as lactate. The separation of lactate and threonine is a challenging task even using editing methods. In the case with potential alterations in threonine, one may consider using a recently proposed J-difference editing with very narrow-bandwidth editing pulse at the high field [57] despite the moderate reproducibility. In addition, the methyl group of β-hydroxybutyrate at 1.19 ppm is close to that of lactate resonance at 1.31 ppm. Under normal physiological conditions, its level is ~ 0.05 μmol/g [58]; therefore, we did not consider it in the current study. For studies under fasting, starvation or ketosis, β-hydroxybutyrate levels may be substantially higher, and it should then be included in the prior knowledge for quantification.

For short-TE protocol, the overlapping short T_2 components, mainly macromolecular resonances, including amino acids such as leucine, isoleucine and valine from different proteins[59], should be carefully handled. In this study, experimentally measured macromolecule spectrum from healthy subjects was included. Similarly, in the phantom study, broad BSA spectra were taken into account in the basis set. In the situation that no lactate is in the phantom, protocol I successfully reported the correct value like the other two protocols. Note that macromolecule spectrum in the brain may differ between different regions or under different pathological states. Therefore, the macromolecule spectrum should be experimentally evaluated and taken into account in the prior knowledge for spectral quantification to avoid potential effect on quantification of metabolites with low abundance. Overall, a complete basis set for quantification in a dedicated application study is crucial, as missing components in the spectral region of lactate may contribute to the "lactate" signal quantified by LCModel or other quantification tools using prior knowledge modeling approach. On the other hand, long TE and inversion protocols are less susceptible to this aspect as the macromolecule spectrum is minimized by relaxation schemes. The

complete elimination of macromolecule resonances can be achieved by editing schemes such as J-difference editing[57] and double-quantum filters[27], although sensitivity and information from other important metabolites are sacrificed.

In addition, the use of OVS module prior to the localization is a prerequisite for high quality spectra without extracranial lipid contamination that could substantially affect lactate measurement especially for the short TE protocol. In applications with the presence of intense lipid signals such as brain tumors and stroke, spectral editing schemes may be more preferable approaches over all three protocols investigated in the current study. The long TE and inversion protocols may not be efficient as the T_1 and T_2 relaxation times of mobile lipids in tumors are longer than normal brain lipids[60].

Moreover, the effect of relaxation times on the signal intensity is an important aspect to consider, as relaxation times are sensitive to changes in the microenvironment and may vary due to aging[61], pathology and across different brain regions. Of the three, protocol I, with short TE and long TR, is the least sensitive protocol to relaxation effects. A 10% alteration in T_2 relaxation will only lead to a 1.5% change in lactate concentration, while for protocol II, a 11.5% change is expected. On the other hand, a 10% shorter T_1 will lead to 1.1% higher values for lactate concentrations measured by protocol I and II, but 28.7% higher values when using protocol III. As research and clinical studies commonly conducting comparisons between groups such as healthy controls vs. patients, the knowledge of relaxation times for individual groups is critical for protocol II and III and additional measurements of relaxation times are required.

Concentrations of metabolites such as glutamate, glutamine, γ-aminobutyric and glutathione can provide important information on the pathophysiology of psychiatric and neurologic diseases [62] and also insights into mechanisms underlying neuronal activity[29,34]. The three evaluated protocols in our study all offer the possibility for the simultaneous detection of these metabolites with lactate, and *in vivo* measurements demonstrated that all three protocols had potential to measure their concentrations with CRLB < 20%. Glu and GABA had similar measurement uncertainty across all three protocols as indicated by their similar CRLBs (2% for Glu and 13-15% for GABA). Higher CRLBs for Gln and GSH in protocol II (12% for Gln, 16% for GSH) relative to III (6% for Gln and 9% for GSH) and I (9% for Gln and 7% for GSH) may be ascribed to J-evolution at long TE worsening the quality of quantification for these two J-coupled metabolites.

Several test-retest studies investigated the reproducibility of GABA, GSH, Gln and Glu by non-editing (STEAM and semi-LASER) and editing techniques (for GABA and GSH) in different brain regions and with various measurement parameters at 7T (summarized in Supporting Information Table S1). The CRLBs of GABA, GSH, Glu and Gln measured by protocol I and III are well in the range of these

published studies at 7T [63–67]. Protocol II has in general the highest CRLBs and within-session CVs for most of the metabolites including Glu, Gln, GSH, and Lac, therefore its reliability is the poorest among three protocols. In the contrary, short TE is the most robust protocol as a general good reproducibility can be reached for all metabolites of interests (Table 2). In this study within-session CVs for GSH using protocol I (8.2 ± 6.6%) are comparable with previous test-retest CVs for both J-difference editing method (7.8 ± 3.2%) and non-editing methods (STEAM, 5%; semi-LASER, 9%; STEAM with inversion: 11.6 ± 5.1%) [64,66-67]. Test-retest CVs of GABA have been previously assessed for editing methods (3.6-16.9%) [63,65,67] and non-editing methods (3.5-17%) [63,66-67]. The mean within-session CVs of GABA in the present study was 11.7% for protocol I, which is within the range of previous studies. Nevertheless, CVs of GABA using protocol II and especially III were unacceptably high. Therefore, GABA measurement is compromised when using protocol II and III, although good reproducibility can be achieved for Lac and Gln using protocol III.

Furthermore, The measurement accuracy of all these metabolites of interest depended on the spectral linewidth and SNR (Supporting Information Figure S4), which is consistent as the observation in another study of GABA at 3T[54]. Therefore, the respective measurement bias should be considered when performing absolute quantification and matched spectral quality must be strictly controlled for studies with group comparison.

Conclusions

Short-TE and inversion recovery protocols have the potential to measure lactate at 7T with good reproducibility. However, lactate levels were underestimated by all three protocols with long TE protocol having the greatest underestimation and measurement variance. As measurement accuracy and precision depend on spectral linewidth and SNR, matched spectral quality is important for group comparisons. Moreover, simulation is valuable for the optimization of measurement protocols in future study design and the correction for measurement bias.

Abbreviations used

Glutamate (Glu), glutamine (Gln), glutathione (GSH), γ-aminobutyric acid (GABA), semi-adiabatic spin-echo full-intensity localized spectroscopy (semi-adiabatic SPECIAL), volume of interest (VOI), outer volume suppression (OVS), N-acetylaspartate (NAA), creatine (Cr), phosphocreatine (PCr), reproducibility error (RE), estimation error (EE), macromolecule (MM), Cramér-Rao lower bound (CRLB), SNR (signal to noise), TE (echo time), TI (inversion time), lactate (Lac).

Figure legend

Figure 1. T_1-weighted images acquired using MP2RAGE (TE/TR = 4.94/6000 ms, TI_1/TI_2 = 800/2700 ms, voxel size = 0.6 x 0.6 x 0.6 mm^3, matrix size = 320 × 320 × 256). Voxel of interest (VOI = 30 × 15 × 15 $mm^{3)}$ for acquisition of MRS data was placed in the right dorsolateral prefrontal cortex (DLPFC).

Figure 2. Representative *in vivo* ^{1}H spectra of the right DLPFC (VOI = 30 × 15 × 15 mm^3) acquired using the semi-adiabatic SPECIAL sequence with (a) protocol I. TE = 16 ms, no inversion, (b) protocol II. TE = 110 ms, no inversion, and (c) protocol III. TE = 16 ms, TI = 300 ms. Individual fits from LCModel were shown for lactate (Lac), glutamate (Glu), glutamine (Gln), γ-aminobutyric acid (GABA), glutathione (GSH), and macromolecule (MM). On top of each spectrum, the area around the lactate peak at 1.3 ppm was enlarged for better visualization.

Figure 3. The *in vivo* lactate concentration estimated using three protocols I. TE = 16 ms, no inversion, II. TE = 110 ms, no inversion, and III. TE = 16 ms, TI = 300 ms based on the semi-adiabatic SPECIAL sequence. The mean lactate concentrations were shown with horizontal bars.

Figure 4. The dependence of (A) lactate concentration and (B) CRLB (%) on spectral SNR when using three protocols in vivo. Protocol I: TE = 16 ms, no inversion (○); II: TE = 110 ms, no inversion (□); III: TE = 16 ms, TI= 300 ms (Δ). Each data point showed the value obtained from spectra with 20 averages (blank), 40 averages (filled grey), and 60 averages (filled black). The standard deviations were shown as error bars for each data point.

Figure 5. Top: Example of simulated spectra for three protocols (a) I. TE = 16 ms, no inversion, (b) II. TE = 110 ms, no inversion, and (c) III. TE = 16 ms, TI = 300 ms at spectral SNRs obtained at the experimental conditions with the same acquisition time (SNR 300 for protocol I and 150 for protocols II and III) and different linewidth (LW). Bottom: LCModel fits of baseline, macromolecule spectrum and lactate for each protocol.

Figure 6 . Contour plots of mean estimation error (EE %) (a), mean reproducibility error (b), and mean Cramér–Rao lower bound (CRLB) (c) for lactate as a function of spectral linewidth and SNR for three protocols (left, middle, right).

Figure 7. Mean estimation error (EE %) of lactate, as a function of spectral linewidth at the experimental SNR. SNR of 300 for protocol I (TE = 16 ms, no inversion). SNR of 150 for protocols II (TE = 110 ms, no inversion) and III (TE = 16 ms, TI = 300 ms).

Figure 8. (A) Phantom lactate concentrations measured by three protocols versus the actual lactate concentrations in the phantoms. The dotted line represents a reference line with a slope of 1. Solid lines are linear fits of values measured by three protocols. The slopes are 0.87 (R^2 = 0.9947), 0.69 (R^2 = 0.9968) and 0.83 (R^2 = 9688) for protocol I, II and III, respectively. Overall, phantom lactate levels were underestimated by all three protocols, to the most extent when using protocol II, which is consistent with the simulation results. Measured lactate levels from phantom spectra with different spectral linewidth (B) and number of averages (C). Lactate concentrations vary with the spectral linewidth while less with the spectral SNR.

Supporting Information Figure S1. (a) Signal intensity of lactate as a function of TE (T_2 relaxation effect is included) and (b) the corresponding spectra of lactate methyl (CH_3) resonance at TE of 110ms (blue) and 144ms (black).

Supporting Information Figure S2. MR spectra of phantoms (4% BSA, 4mM creatine,0.2mM Lac) measured by three protocols and the respective fits of BSA and lactate.

Supporting Information Figure S3. Contour plot of mean **Cramér–Rao lower bound (CRLB)** for glutamate(Glu), glutamine(Gln), γ-aminobutyric acid (GABA), and glutathione (GSH) as a function of linewidth and SNR for the three protocols (a) I. TE = 16 ms, no inversion, (b) II. TE = 110 ms, no inversion, and (c) III. TE = 16 ms, TI = 300 ms.

Supporting Information Figure S4..Contour plot of **mean estimation error (EE %)** for glutamate(Glu), glutamine(Gln), γ-aminobutyric acid (GABA), and glutathione (GSH) as a function of linewidth and SNR for the three protocols (a) I. TE = 16 ms, no inversion, (b) II. TE = 110 ms, no inversion, and (c) III. TE = 16 ms, TI = 300 ms.

Supporting Information Figure S5. Contour plot of **mean reproducibility error (RE%)** for glutamate(Glu), glutamine(Gln), γ-aminobutyric acid (GABA), and glutathione (GSH) as a function of linewidth and SNR for the three protocols (a) I. TE = 16 ms, no inversion, (b) II. TE = 110 ms, no inversion, and (c) III. TE = 16 ms, TI = 300 ms.

Supporting Information Table S1. Summary of reproducibility studies of GABA, GSH, Gln and Glu at 7T.

Table 1. Apparent concentrations and CRLB of metabolites measured *in vivo* (n = 7) using three protocols I. TE = 16 ms, no inversion, II. TE = 110 ms, no inversion, and III. TE = 16 ms, TI = 300 ms for the semi-adiabatic SPECIAL sequence. All experimentally measured values were listed as mean ± SD.

Metabolite	Apparent concentration [-] and CRLB [%]					
	Protocol I	CRLB	Protocol II	CRLB	Protocol III	CRLB
Alanine	0.43 [54]	-	0.18 *	-	0.08 ± 0.10	128 ±131
Ascorbate	1.12 [55]	-	0.85 ± 0.25	14 ± 3	0.62 *	-
Aspartate	0.84 ± 0.21	22 ± 9	1.08 ± 0.17	8 ± 1	0.51 ± 0.19	23 ± 10
Creatine	2.33 ± 0.25	4 ± 1	(CH_3) 1.28 ± 0.69	13 ± 9	(CH_3) 1.35 ± 0.56	16 ± 5
			(CH_2) 0.70 ± 0.14	9 ± 3	(CH_2) 0.67 ± 0.20	9 ± 3
Glucose	0.86 [54]	-	0.17 ± 0.06	64 ± 30	0.56 *	-
Glycerophosphocholine	0.46 ± 0.15	14 ± 8	0.13 ± 0.08	38 ± 30	0.34 ± 0.07	4 ± 1
Glycine	0.38 ± 0.14	18 ± 4	0.16 *	-	0.22 ± 0.07	19 ± 10
Glutamate	6.37 ± 0.48	2 ± 0	2.74 ± 0.36	2 ± 0	3.51 ± 0.63	2 ± 0
Glutamine	1.04 ± 0.43	9 ± 3	0.49 ± 0.14	12 ± 3	0.95 ± 0.26	6 ± 2
Glutathione	0.55 ± 0.13	7 ± 1	0.17 ± 0.04	16 ± 3	0.30 ± 0.08	9 ± 2
Lactate	0.54 ± 0.08	8 ± 1	0.17 ± 0.05	13 ± 3	0.38 ± 0.05	7 ± 1
Myo-inositol	2.75 ± 0.47	3 ± 1	1.20 ± 0.22	4 ± 1	1.47 ± 0.34	3 ± 1
Macromolecule	1.42 ± 0.04	1 ± 0	0.03 ± 0.01	7 ± 1	0.19 ± 0.03	5 ± 1
N-acetylaspartate	9.04 ± 0.50	1 ± 0	(CH_3) 5.39 ± 0.54	1 ± 0	(CH_3) 5.14 ± 0.80	1 ± 0
			(CH_2) 4.27 ± 0.51	3 ± 1	(CH_2) 3.37 ± 0.63	4 ± 1
N-acetylaspartylglutamate	0.89 ± 0.24	8 ± 3	0.26 ± 0.08	16 ± 11	0.40 ± 0.09	10 ± 3
Phosphocholine	0.27 ± 0.23	93 ±156	0.30 ± 0.12	13 ± 12	0.15 *	-
Phosphocreatine	1.66 ± 0.08	5 ± 1	(CH_3) 1.06 ± 0.60	28 ± 39	(CH_3) 1.05 ± 0.55	32 ± 33
			(CH_2) 0.53 ± 0.14	12 ± 4	(CH_2) 0.19 ± 0.17	69 ± 76
Phosphoethanolamine	1.76 ± 0.17	5 ± 1	0.80 ± 0.47	41 ± 19	0.44 ± 0.11	17 ± 6
Serine	0.35 [54]	-	0.15 *	127 ± 94	0.28 ± 0.11	32 ± 16
Scyllo-inositol	0.12 ± 0.05	19 ± 7	0.05 ± 0.03	32 ± 25	0.08 ± 0.04	20 ± 15
Taurine	0.66 ± 0.12	11 ± 1	0.25 ± 0.07	19 ± 10	0.60 ± 0.15	7 ± 2
γ-Aminobutyric acid	0.80 ± 0.18	13 ± 3	0.22 ± 0.04	15 ± 2	0.55± 0.23	15 ± 7

*Estimated based on the value used in protocol I with relaxation effects.

Table 2. Within-session coefficients of variance (CVs) of metabolites of interest (n=7).

| CV(%)	Lac	Glu	Gln	GSH	GABA
Protocol I	6.1 ± 7.9	1.0 ± 0.5	6.2 ± 3.0	8.2 ± 6.6	11.7 ± 8.4
Protocol II	22.3 ± 12.3	4.4 ± 4.0	13.4 ± 13.3	13.4 ± 23.1	16.5 ± 9.6
Protocol III	5.1 ± 5.4	2.5 ± 2.1	4.8 ± 4.7	14.5 ± 13.2	39.4 ± 32.2*

*Not detectable in the sub-sessions of two subjects.

References

1. Brooks GA. Lactate shuttles in nature. Biochem Soc Trans. 2002;30(2):258-264. doi:10.1042.

2. Gladden LB. Lactate metabolism: a new paradigm for the third millennium. J Physiol. 2004;558(1):5-30. doi:10.1113/jphysiol.2003.058701.

3. Schurr A. Lactate: the ultimate cerebral oxidative energy substrate? J Cereb Blood Flow Metab. 2006;26(1):142-152. doi:10.1038/sj.jcbfm.9600174.

4. Magistretti PJ, Allaman I. A cellular perspective on brain energy metabolism and functional imaging. Neuron. 2015;86(4):883-901. doi:10.1016/j.neuron.2015.03.035.

5. Dennis A, Thomas AG, Rawlings NB, et al. An Ultra-High Field Magnetic Resonance Spectroscopy Study of Post Exercise Lactate, Glutamate and Glutamine Change in the Human Brain. Front Physiol. 2015;6. doi:10.3389/fphys.2015.00351.

6. Maddock RJ, Casazza GA, Buonocore MH, Tanase C. Vigorous exercise increases brain lactate and Glx (glutamate+glutamine): a dynamic ^{1}H-MRS study. NeuroImage. 2011;57(4):1324-1330. doi:10.1016/j.neuroimage.2011.05.048.

7. Prichard J, Rothman D, Novotny E, et al. Lactate rise detected by ^{1}H NMR in human visual cortex during physiologic stimulation. Proc Natl Acad Sci U S A. 1991;88(13):5829-5831.

8. Sappey-Marinier D, Calabrese G, Fein G, Hugg JW, Biggins C, Weiner MW. Effect of photic stimulation on human visual cortex lactate and phosphates using ^{1}H and ^{31}P magnetic resonance spectroscopy. J Cereb Blood Flow Metab. 1992;12(4):584-592. doi:10.1038/jcbfm.1992.82.

9. Friedman SD, Jensen JE, Frederick BB, Artru AA, Renshaw PF, Dager SR. Brain changes to hypocapnia using rapidly interleaved phosphorus-proton magnetic resonance spectroscopy at 4 T. J Cereb Blood Flow Metab. 2007;27(3):646-653. doi:10.1038/sj.jcbfm.9600383.

10. van Rijen PC, Luyten PR, van der Sprenkel JW, et al. ^{1}H and ^{31}P NMR measurement of cerebral lactate, high-energy phosphate levels, and pH in humans during voluntary hyperventilation: associated EEG, capnographic, and Doppler findings. Magn Reson Med. 1989;10(2):182-193.

11. Chu W-J, Delbello MP, Jarvis KB, et al. Magnetic resonance spectroscopy imaging of lactate in patients with bipolar disorder. Psychiatry Res. 2013;213(3):230-234. doi:10.1016/j.pscychresns.2013.03.004

12. Dager SR, Friedman SD, Parow A, et al. Brain metabolic alterations in medication-free patients with bipolar disorder. Arch Gen Psychiatry. 2004;61(5):450-458. doi:10.1001/archpsyc.61.5.450.

13. Machado-Vieira R, Zanetti MV, Otaduy MC, et al. Increased Brain Lactate During Depressive Episodes and Reversal Effects by Lithium Monotherapy in Drug-Naive Bipolar Disorder: A 3-T ^{1}H-MRS Study. J Clin Psychopharmacol. 2017;37(1):40-45. doi:10.1097/JCP.0000000000000616

14. Xu J, Dydak U, Harezlak J, et al. Neurochemical abnormalities in unmedicated bipolar depression and mania: a 2D ^{1}H MRS investigation. Psychiatry Res. 2013;213(3):235-241. doi:10.1016/j.pscychresns.2013.02.008

15. Ernst J, Hock A, Henning A, Seifritz E, Boeker H, Grimm S. Increased pregenual anterior cingulate glucose and lactate concentrations in major depressive disorder. Mol Psychiatry. 2017;22(1):113-119. doi:10.1038/mp.2016.73

16. Maddock RJ. The lactic acid response to alkalosis in panic disorder: an integrative review. J Neuropsychiatry Clin Neurosci. 2001;13(1):22-34. doi:10.1176/jnp.13.1.22

17. Maddock RJ, Buonocore MH, Copeland LE, Richards AL. Elevated brain lactate responses to neural activation in panic disorder: a dynamic ^{1}H-MRS study. Mol Psychiatry. 2009;14(5):537-545. doi:10.1038/sj.mp.4002137

18. Rowland LM, Pradhan S, Korenic S, et al. Elevated brain lactate in schizophrenia: a 7 T magnetic resonance spectroscopy study. Transl Psychiatry. 2016;6(11):e967. doi:10.1038/tp.2016.239

19. Lin DDM, Crawford TO, Barker PB. Proton MR spectroscopy in the diagnostic evaluation of suspected mitochondrial disease. AJNR Am J Neuroradiol. 2003;24(1):33-41.

20. Sijens PE, Levendag PC, Vecht CJ, van Dijk P, Oudkerk M. 1H MR spectroscopy detection of lipids and lactate in metastatic brain tumors. NMR Biomed. 1996;9(2):65-71.

21. Mathews VP, Barker PB, Blackband SJ, Chatham JC, Bryan RN. Cerebral metabolites in patients with acute and subacute strokes: concentrations determined by quantitative proton MR spectroscopy. AJR Am J Roentgenol. 1995;165(3):633-638. doi:10.2214/ajr.165.3.7645484.

22. Mangia S, Tkác I, Gruetter R, Van de Moortele P-F, Maraviglia B, Uğurbil K. Sustained neuronal activation raises oxidative metabolism to a new steady-state level: evidence from 1H NMR spectroscopy in the human visual cortex. J Cereb Blood Flow Metab Off J Int Soc Cereb Blood Flow Metab. 2007;27(5):1055-1063. doi:10.1038/sj.jcbfm.9600401.

23. Schaller B, Xin L, O'Brien K, Magill AW, Gruetter R. Are glutamate and lactate increases ubiquitous to physiological activation? A (1)H functional MR spectroscopy study during motor activation in human brain at 7Tesla. NeuroImage. 2014;93 Pt 1:138-145. doi:10.1016/j.neuroimage.2014.02.016.

24. Arteaga de Castro CS, Boer VO, Andreychenko A, et al. Improved efficiency on editing MRS of lactate and γ-aminobutyric acid by inclusion of frequency offset corrected inversion pulses at high fields: MRS EDITING WITH FOCI PULSES AT 7 T. NMR Biomed. 2013;26(10):1213-1219. doi:10.1002/nbm.2937.

25. Smith MA, Koutcher JA, Zakian KL. J-difference lactate editing at 3.0 Tesla in the presence of strong lipids. J Magn Reson Imaging JMRI. 2008;28(6):1492-1498. doi:10.1002/jmri.21584.

26. Star-Lack J, Spielman D, Adalsteinsson E, Kurhanewicz J, Terris DJ, Vigneron DB. In vivo lactate editing with simultaneous detection of choline, creatine, NAA, and lipid singlets at 1.5 T using PRESS excitation with applications to the study of brain and head and neck tumors. J Magn Reson San Diego Calif 1997. 1998;133(2):243-254. doi:10.1006/jmre.1998.1458.

27. Boer VO, Luijten PR, Klomp DWJ. Refocused double-quantum editing for lactate detection at 7 T. Magn Reson Med. 2013;69(1):1-6. doi:10.1002/mrm.24227.

28. Emir UE, Auerbach EJ, Van De Moortele P-F, et al. Regional Neurochemical Profiles in the Human Brain measured by ^{1}H MRS at 7 Tesla using Local B1 Shimming. NMR Biomed. 2012;25(1):152-160. doi:10.1002/nbm.1727

29. Lin Y, Stephenson MC, Xin L, Napolitano A, Morris PG. Investigating the Metabolic Changes due to Visual Stimulation using Functional Proton Magnetic Resonance Spectroscopy at 7 T. J Cereb Blood Flow Metab. 2012;32(8):1484-1495. doi:10.1038/jcbfm.2012.33.

30. Mangia S, Tkác I, Gruetter R, et al. Sensitivity of single-voxel ^{1}H-MRS in investigating the metabolism of the activated human visual cortex at 7 T. Magn Reson Imaging. 2006;24(4):343-348. doi:10.1016/j.mri.2005.12.023.

31. Mekle R, Mlynárik V, Gambarota G, Hergt M, Krueger G, Gruetter R. MR spectroscopy of the human brain with enhanced signal intensity at ultrashort echo times on a clinical platform at 3T and 7T. Magn Reson Med. 2009;61(6):1279-1285. doi:10.1002/mrm.21961.

32. Tkác I, Oz G, Adriany G, Uğurbil K, Gruetter R. In vivo ^{1}H NMR spectroscopy of the human brain at high magnetic fields: metabolite quantification at 4T vs. 7T. Magn Reson Med. 2009;62(4):868-879. doi:10.1002/mrm.22086.

33. Duarte JMN, Xin L. Magnetic Resonance Spectroscopy in Schizophrenia: Evidence for Glutamatergic Dysfunction and Impaired Energy Metabolism. Neurochem Res. 2019;44(1):102-116. doi:10.1007/s11064-018-2521-z.

34. Schaller B, Mekle R, Xin L, Kunz N, Gruetter R. Net increase of lactate and glutamate concentration in activated human visual cortex detected with magnetic resonance spectroscopy at 7 tesla. J Neurosci Res. 2013;91(8):1076-1083. doi:10.1002/jnr.23194.

35. Bednařík P, Tkáč I, Giove F, et al. Neurochemical responses to chromatic and achromatic stimuli in the human visual cortex. J Cereb Blood Flow Metab Off J Int Soc Cereb Blood Flow Metab. 2018;38(2):347-359. doi:10.1177/0271678X17695291.

36. Provencher S. LCModel & LCMgui User's Manual. 2019. http://s-provencher.com/pub/LCModel/manual/manual.pdf.

37. Stefan D, Cesare FD, Andrasescu A, et al. Quantitation of magnetic resonance spectroscopy signals: the jMRUI software package. Meas Sci Technol. 2009;20(10):104035. doi:10.1088/0957-0233/20/10/104035

38. Xin L, Schaller B, Mlynarik V, Lu H, Gruetter R. Proton T1 relaxation times of metabolites in human occipital white and gray matter at 7 T. Magn Reson Med. 2013;69(4):931-936. doi:10.1002/mrm.24352

39. Adalsteinsson E, Spielman DM, Wright GA, Pauly JM, Meyer CH, Macovski A. Incorporating lactate/lipid discrimination into a spectroscopic imaging sequence. Magn Reson Med. 1993;30(1):124-130. doi:10.1002/mrm.1910300119

40. Frahm J, Bruhn H, Gyngell ML, Merboldt KD, Hänicke W, Sauter R. Localized proton NMR spectroscopy in different regions of the human brain in vivo. Relaxation times and concentrations of cerebral metabolites. Magn Reson Med. 1989;11(1):47-63.

41. Guillozet-Bongaarts AL, Hyde TM, Dalley RA, et al. Altered gene expression in the dorsolateral prefrontal cortex of individuals with schizophrenia. Mol Psychiatry. 2014;19(4):478-485. doi:10.1038/mp.2013.30.

42. Pennington K, Beasley CL, Dicker P, et al. Prominent synaptic and metabolic abnormalities revealed by proteomic analysis of the dorsolateral prefrontal cortex in schizophrenia and bipolar disorder. Mol Psychiatry. 2008;13(12):1102-1117. doi:10.1038/sj.mp.4002098.

43. Callicott JH, Bertolino A, Mattay VS, et al. Physiological dysfunction of the dorsolateral prefrontal cortex in schizophrenia revisited. Cereb Cortex N Y N 1991. 2000;10(11):1078-1092.

44. Koenigs M, Grafman J. The functional neuroanatomy of depression: Distinct roles for ventromedial and dorsolateral prefrontal cortex. Behav Brain Res. 2009;201(2):239-243. doi:10.1016/j.bbr.2009.03.004

45. Sullivan CR, Koene RH, Hasselfeld K, O'Donovan SM, Ramsey A, McCullumsmith RE. Neuron-specific deficits of bioenergetic processes in the dorsolateral prefrontal cortex in schizophrenia. Mol Psychiatry. March 2018:1. doi:10.1038/s41380-018-0035-3.

46. Teeuwisse WM, Brink WM, Haines KN, Webb AG. Simulations of high permittivity materials for 7 T neuroimaging and evaluation of a new barium titanate-based dielectric. Magn Reson Med. 2012;67(4):912-918. doi:10.1002/mrm.24176.

47. Marques JP, Kober T, Krueger G, van der Zwaag W, Van de Moortele P-F, Gruetter R. MP2RAGE, a self bias-field corrected sequence for improved segmentation and T1-mapping at high field. NeuroImage. 2010;49(2):1271-1281. doi:10.1016/j.neuroimage.2009.10.002.

48. Gruetter R, Tkác I. Field mapping without reference scan using asymmetric echo-planar techniques. Magn Reson Med. 2000;43(2):319-323.

49. Tkác I, Starcuk Z, Choi IY, Gruetter R. In vivo 1H NMR spectroscopy of rat brain at 1 ms echo time. Magn Reson Med. 1999;41(4):649-656.

50. Xin L, Gambarota G, Mlynárik V, Gruetter R. Proton T2 relaxation time of J-coupled cerebral metabolites in rat brain at 9.4 T. NMR Biomed. 2008;21(4):396-401. doi:10.1002/nbm.1205.

51. Schaller B, Xin L, Gruetter R. Is the macromolecule signal tissue-specific in healthy human brain? A (1)H MRS study at 7 Tesla in the occipital lobe. Magn Reson Med. 2014;72(4):934-940. doi:10.1002/mrm.24995.

52. Naressi A, Couturier C, Devos JM, et al. Java-based graphical user interface for the MRUI quantitation package. Magma N Y N. 2001;12(2-3):141-152.

53. Marjańska M, Auerbach EJ, Valabrégue R, Van de Moortele P-F, Adriany G, Garwood M. Localized 1H NMR Spectroscopy in Different Regions of Human Brain In Vivo at 7 T: T2 Relaxation Times and Concentrations of Cerebral Metabolites. NMR Biomed. 2012;25(2):332-339. doi:10.1002/nbm.1754

54. Near J, Andersson J, Maron E, et al. Unedited in vivo detection and quantification of γ-aminobutyric acid in the occipital cortex using short-TE MRS at 3 T. NMR Biomed. 2013;26(11):1353-1362. doi:10.1002/nbm.2960.

55. Terpstra M, Gruetter R. 1H NMR detection of vitamin C in human brain in vivo. Magn Reson Med. 2004;51(2):225-229. doi:10.1002/mrm.10715.

56. Sadler PJ, Tucker A. Proton NMR studies of bovine serum albumin. Eur J Biochem. 1992;205(2):631-643. doi:10.1111/j.1432-1033.1992.tb16821.x.

57. Wijnen JP, Haarsma J, Boer VO, et al. Detection of lactate in the striatum without contamination of macromolecules by J-difference editing MRS at 7T. NMR Biomed. 2015;28(4):514-522. doi:10.1002/nbm.3278.

58. Pan JW, Rothman TL, Behar KL, Stein DT, Hetherington HP. Human brain beta-hydroxybutyrate and lactate increase in fasting-induced ketosis. J Cereb Blood Flow Metab Off J Int Soc Cereb Blood Flow Metab. 2000;20(10):1502-1507. doi:10.1097/00004647-200010000-00012.

59. Behar KL, Ogino T. Characterization of macromolecule resonances in the 1H NMR spectrum of rat brain. Magn Reson Med. 1993;30(1):38-44. doi:10.1002/mrm.1910300107.

60. Bogner W, Hangel G, Esmaeili M, Andronesi OC. 1D-spectral editing and 2D multispectral in vivo 1H-MRS and 1H-MRSI - Methods and applications. Anal Biochem. 2017;529:48-64. doi:10.1016/j.ab.2016.12.020.

61. Marjańska M, McCarten JR, Hodges J, et al. Region-specific aging of the human brain as evidenced by neurochemical profiles measured noninvasively in the posterior cingulate cortex and the occipital lobe using 1H magnetic resonance spectroscopy at 7 T. Neuroscience. 2017;354:168-177. doi:10.1016/j.neuroscience.2017.04.035.

62. Carlos Zarate J. Glutamatergic Modulators: The Future of Treating Mood Disorders? Harv Rev Psychiatry. 2010;18(5):293. doi:10.3109/10673229.2010.511059.

63. Wijtenburg SA, Rowland LM, Edden RAE, Barker PB. Reproducibility of brain spectroscopy at 7T using conventional localization and spectral editing techniques. J Magn Reson Imaging JMRI. 2013;38(2):460-467. doi:10.1002/jmri.23997.

64. Deelchand DK, Marjańska M, Hodges JS, Terpstra M. Sensitivity and Specificity of Human Brain Glutathione Concentrations Measured Using Short Echo Time 1H MRS at 7 T. *NMR Biomed.* 2016;29(5):600-606. doi:10.1002/nbm.3507

65. Li Y, Bian W, Larson P, et al. Reliable and Reproducible GABA Measurements Using Automated Spectral Prescription at Ultra-High Field. *Front Hum Neurosci*. 2017;11:506. doi:10.3389/fnhum.2017.00506

66. Terpstra M, Cheong I, Lyu T, et al. Test-retest reproducibility of neurochemical profiles with short-echo, single-voxel MR spectroscopy at 3T and 7T. *Magn Reson Med*. 2016;76(4):1083-1091. doi:10.1002/mrm.26022

67. Prinsen H, de Graaf RA, Mason GF, Pelletier D, Juchem C. Reproducibility measurement of glutathione, GABA, and glutamate: Towards in vivo neurochemical profiling of multiple sclerosis with MR spectroscopy at 7T. *J Magn Reson Imaging JMRI*. 2017;45(1):187-198. doi:10.1002/jmri.25356
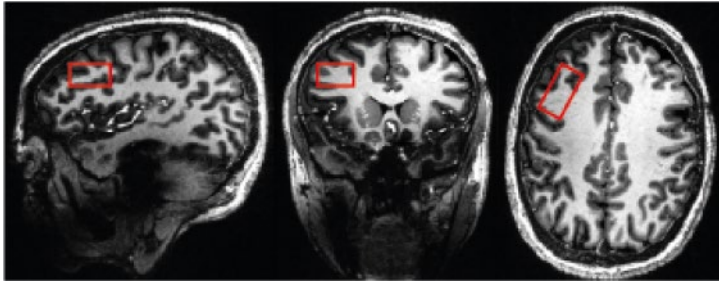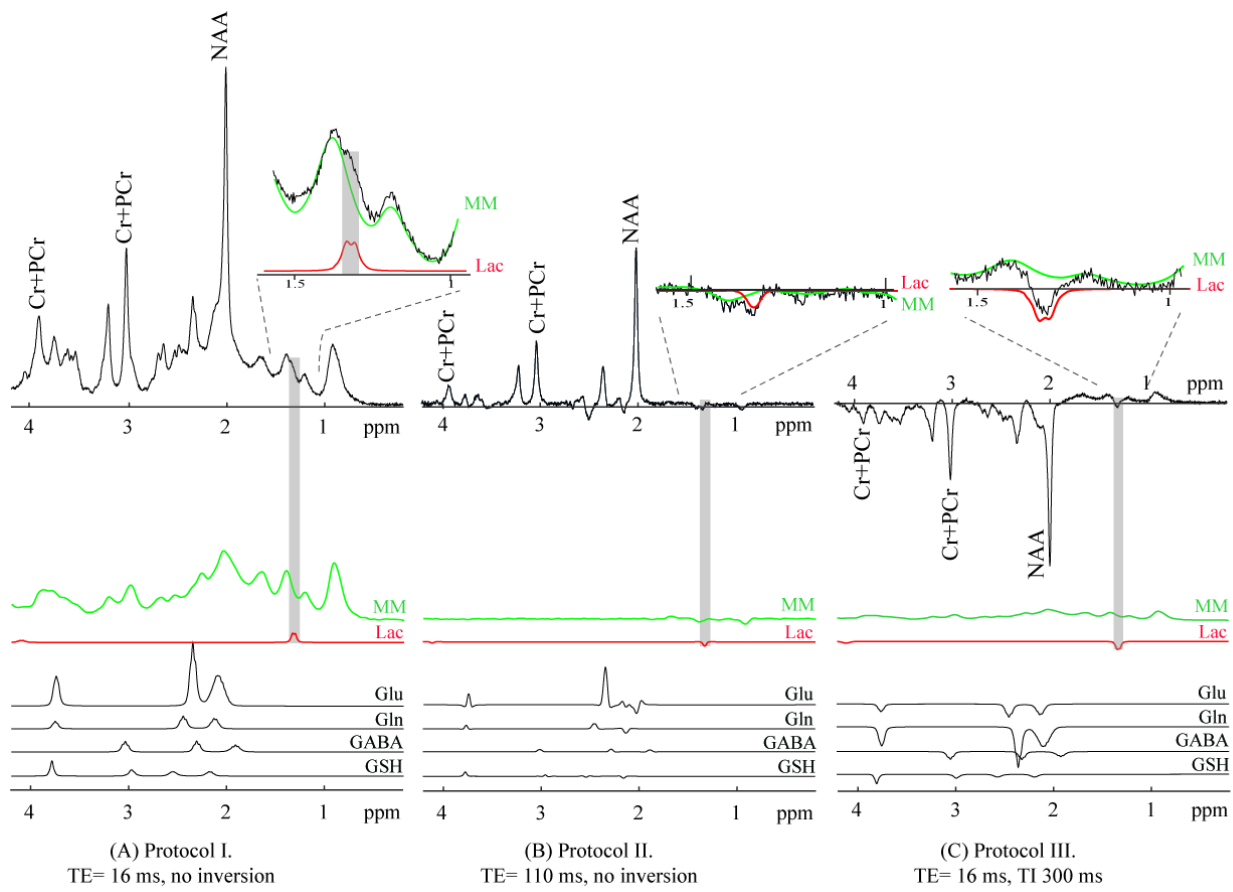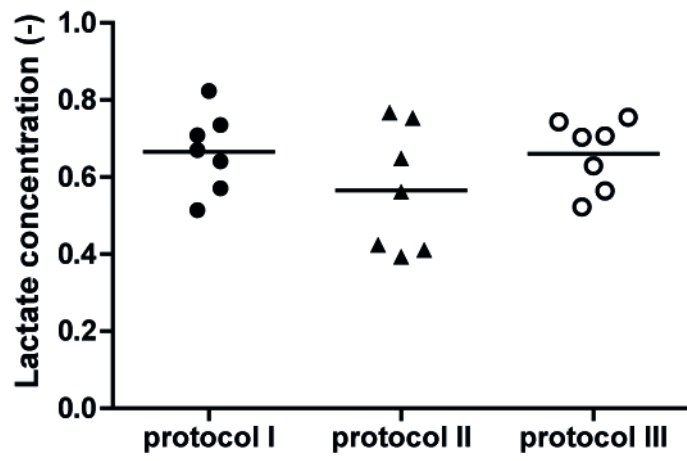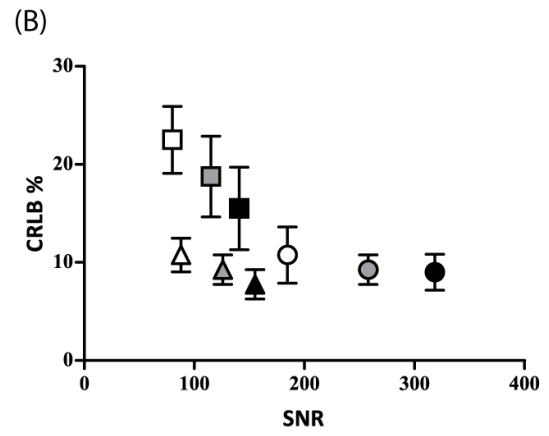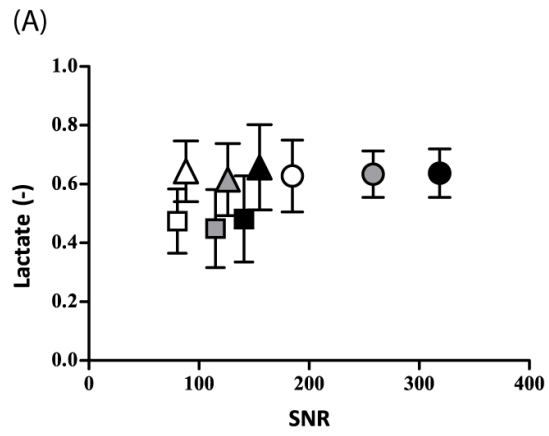
(A) Protocol I.
TE= 16 ms, no inversion

(B) Protocol II.
TE= 110 ms, no inversion

(C) Protocol III.
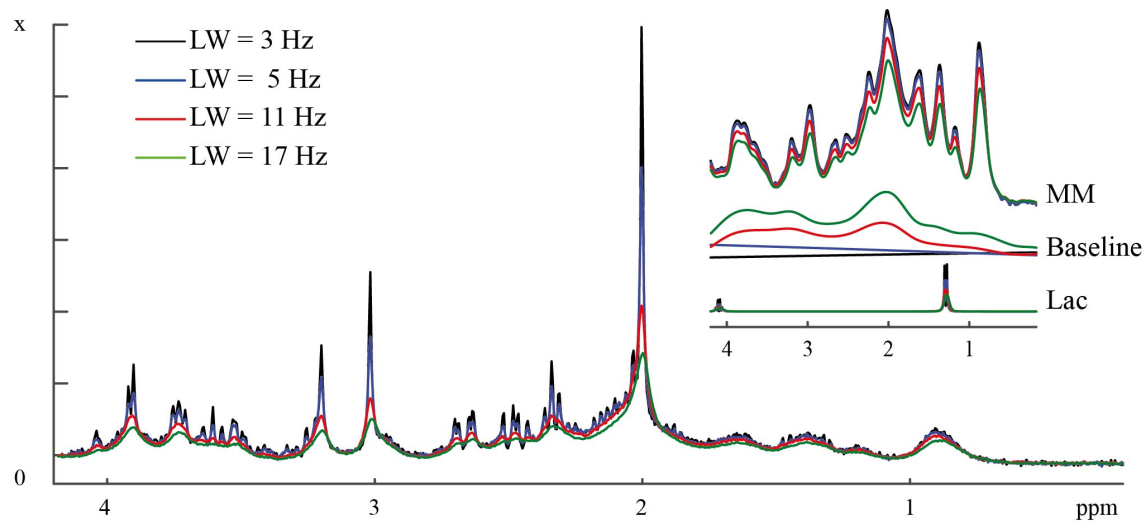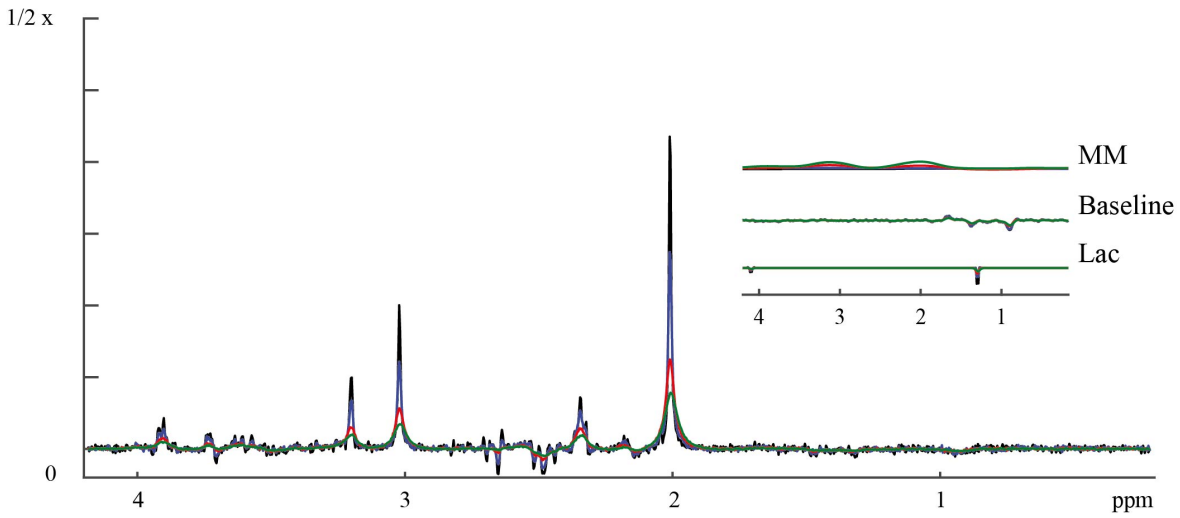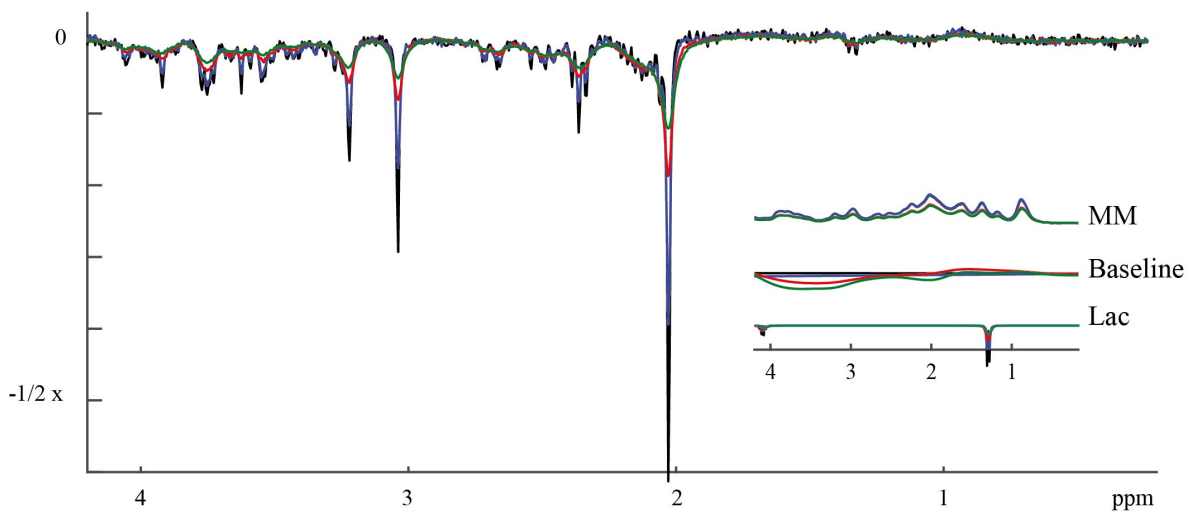TE= 16 ms, TI 300 ms

(A)
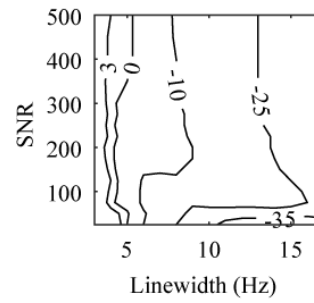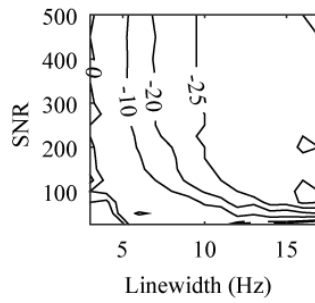

(B)

(A) Protocol I (TE= 16 ms, no inversion)
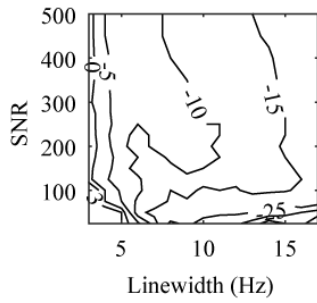
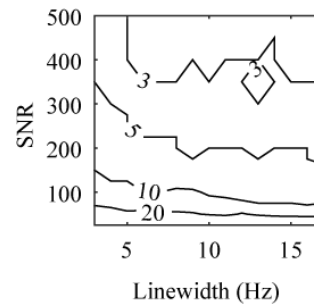(B) Protocol II (TE = 110 ms, no inversion)
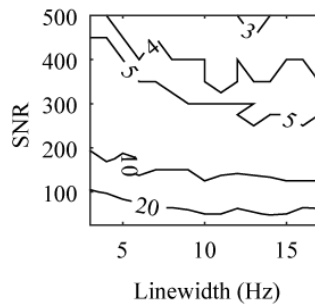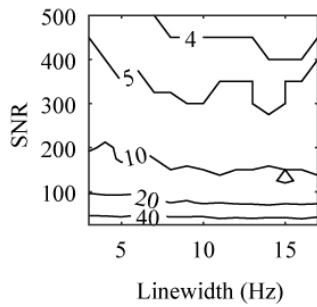
(C) Protocol III (TE = 16 ms, TI = 300 ms)

28

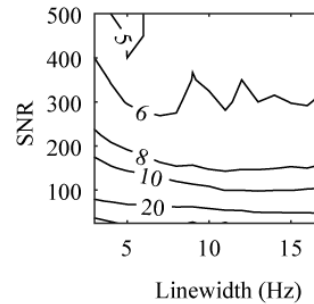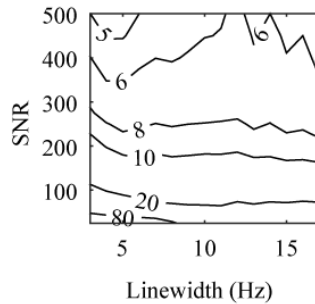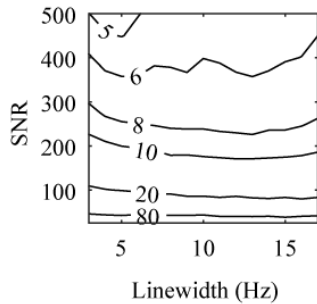Protocol I : TE = 16 ms, no inversion   Protocol II : TE = 110 ms, no inversion   Protocol III : TE = 16 ms, TI = 300 ms

(a) Mean estimation error (%)

(b) Reproducibility error (%)

(c) CRLB (%)

29